Supplementary Materials for Two-dimensional Legendre polynomial method for internal tide signal extraction

In order to demonstrate the effectiveness of the 2-D LPF method in extracting internal tide signals acting on the sea surface, we chose the central basin of the South China Sea (110° E - 120° E, 8° N - 18° N) as another study region for a further research.

Figure S1 illustrates the topography of the study region overlaid with orbit track data. The study region features various complex topographic structures similar to that of the central Indian Ocean region in the article. The temperature and salinity data from January 3 to January 17, 2012, were selected to calculate density perturbations, with the results for the 2th day shown in Figure S2, representing the density perturbation results, with three orbit passing through areas with different density perturbation characteristics. Figure S1 and Figure S2 show the strong correlation between density perturbations and topography, indicating that they both play a significant role in the generation and propagation of internal tides. Figure S3 presents the amplitude and phase lag information of M2 tidal constituent. By examining the amplitude information in the left figure, it is evident that in areas with significant topographic variations and large density perturbations, the continuity of the amplitude is noticeably disrupted. This phenomenon indicates the presence of internal tide signals in these areas.

To demonstrate the effectiveness of the 2-D LPF method in extract the internal tidal signals acting on the sea surface, we compare it with 300 km smooth method and 1-D LPF method. Figure S4 displays the ΔH, ΔG and RMSe extracted using the 2-D LPF method (right part), compared to the results obtained using the 300 km smooth method (left part) and the 1-D LPF method (middle part). The ΔH, ΔG and RMSe values using the 2-D LPF method are generally higher in the study region, specifically in areas between 110° E to 112° E and 8° N to 12° N, indicating a more accurate extraction of internal tide signals. To quantitatively compare the internal tide signals extracted by the 300 km smooth method, the 1-D LPF method and the 2-D LPF method, we perform normal distribution analyses on the internal tide signals obtained by both methods. Additionally, we count the number of signals within different ranges, as illustrated in Figure S5. It is apparent that the 2-D LPF method extracts more valid signals than the 300 km smooth method and the 1-D LPF method.

In order to more accurately assess the effectiveness of 300 km smooth method, 1-D LPF method and 2-D LPF method in extracting internal tide signals. Three distinct orbits are selected for analyzing the correlation between internal tide signals extracted by different method and the density perturbations and topography beneath these orbits, The position of the three orbits are illustrated in in Figure S2. The RMSe, topography, and density perturbations obtained by different methods for three orbits are illustrated in Figure S6. The correlation coefficients between the RMSe derived from different method, and the topography and density perturbations, are shown in Table S1. The results indicate that the correlation coefficients of 2-D LPF method (-0.369, 0.421, -0.178; -0.508, -0.213, 0.214) are generally higher than those obtained by the 300 km smooth (0.045, 0.291, -0.196; 0.017, 0.085,

0.096) and the 1-D LPF method (-0.155, 0.300, -0.184; -0.119, 0.176, 0.095), further proving the accuracy of the 2-D LPF method in extracting internal tide signals.

Contents of this file:

Supplementary Figure S1. Distribution of water depth, satellite orbit paths in the central basin of the South China Sea.

Supplementary Figure S2. The density perturbation results, with three orbit passing through in the central basin of the South China Sea. orbit 1: orange line; orbit 2: yellow line; orbit 3: purple line.

Supplementary Figure S3. Satellite altimeter amplitude data and phase lag data of M2 tidal constituent.

Supplementary Figure S4. Amplitude changes (ΔH), phase lag changes (ΔG) and root mean square errors (RMSe) of the M2 internal tide acting on the sea surface extracted by 300 km smooth method (left part), 1-D LPF method (middle part) and 2-D LPF method (right part).

Supplementary Figure S5. (a) The root mean square errors (RMSe) normal distribution plot of the 300 km smooth method, 1-D LPF method and 2-D LPF method. (b) Comparison of the count of the root mean square errors (RMSe) for the 300 km smooth method, 1-D LPF method and 2-D LPF method at different ranges.

Supplementary Figure S6. The RMSe, topography, and density perturbations obtained by 300 km smooth method, 1-D LPF method and 2-D LPF method for three orbits.

Supplementary Table S1. The correlation coefficients between the RMSe derived from 300 km smooth method, 1-D LPF method, 2-D LPF method, and the topography and density perturbations.
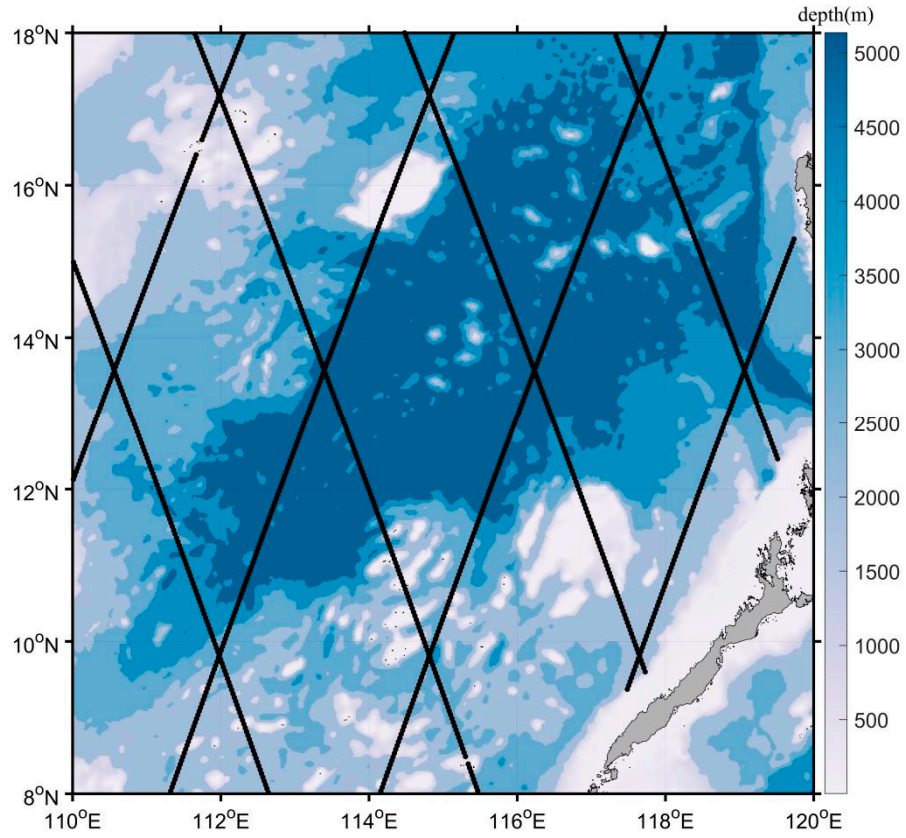
Figure S1. Distribution of water depth, satellite orbit paths in the central basin of the South China Sea.
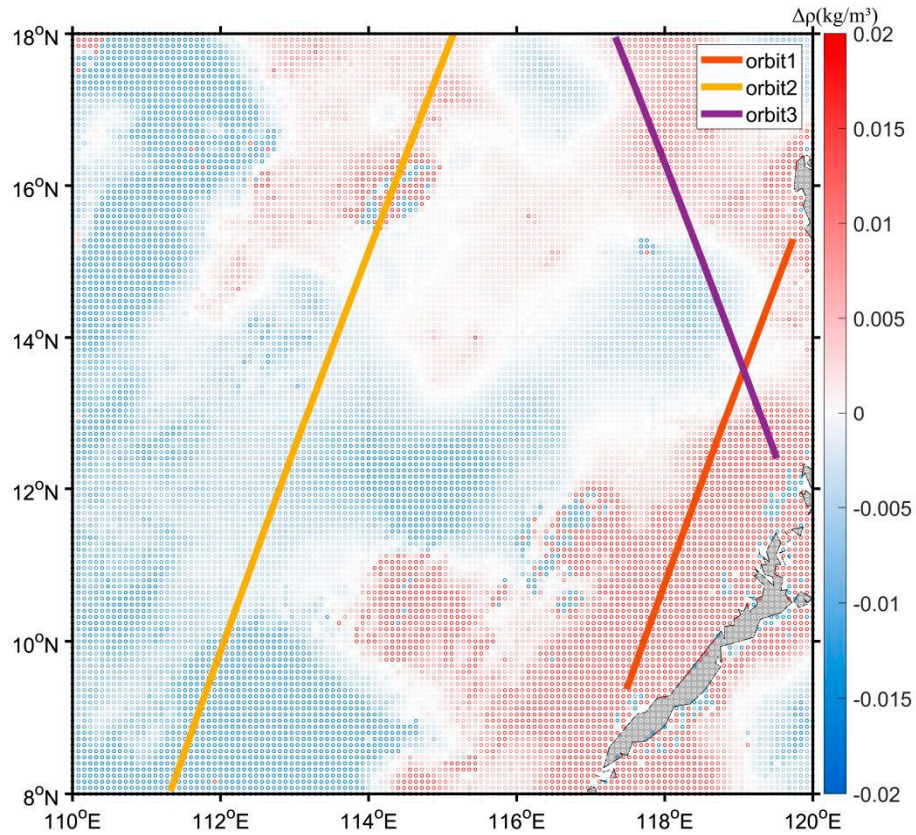

Figure S2. The density perturbation results, with three orbit passing through in the central basin of the South China Sea. orbit 1: orange line; orbit 2: yellow line; orbit 3: purple line.
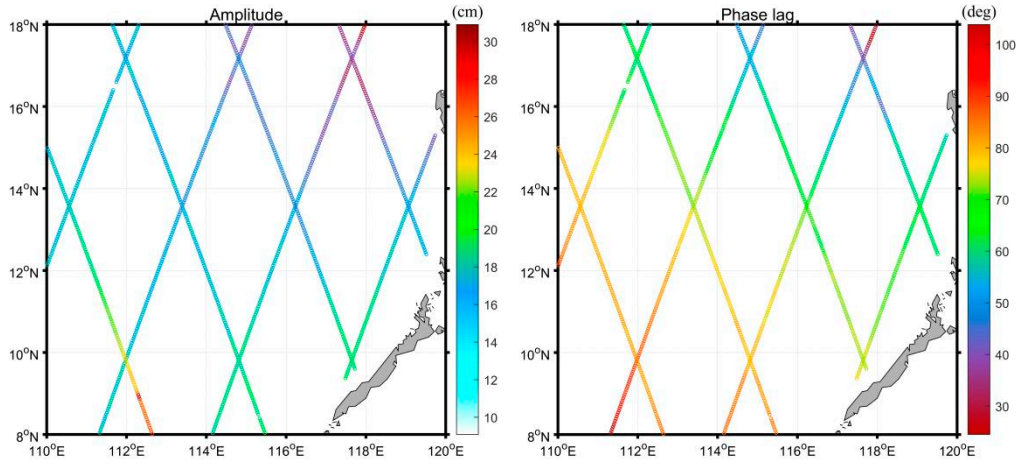
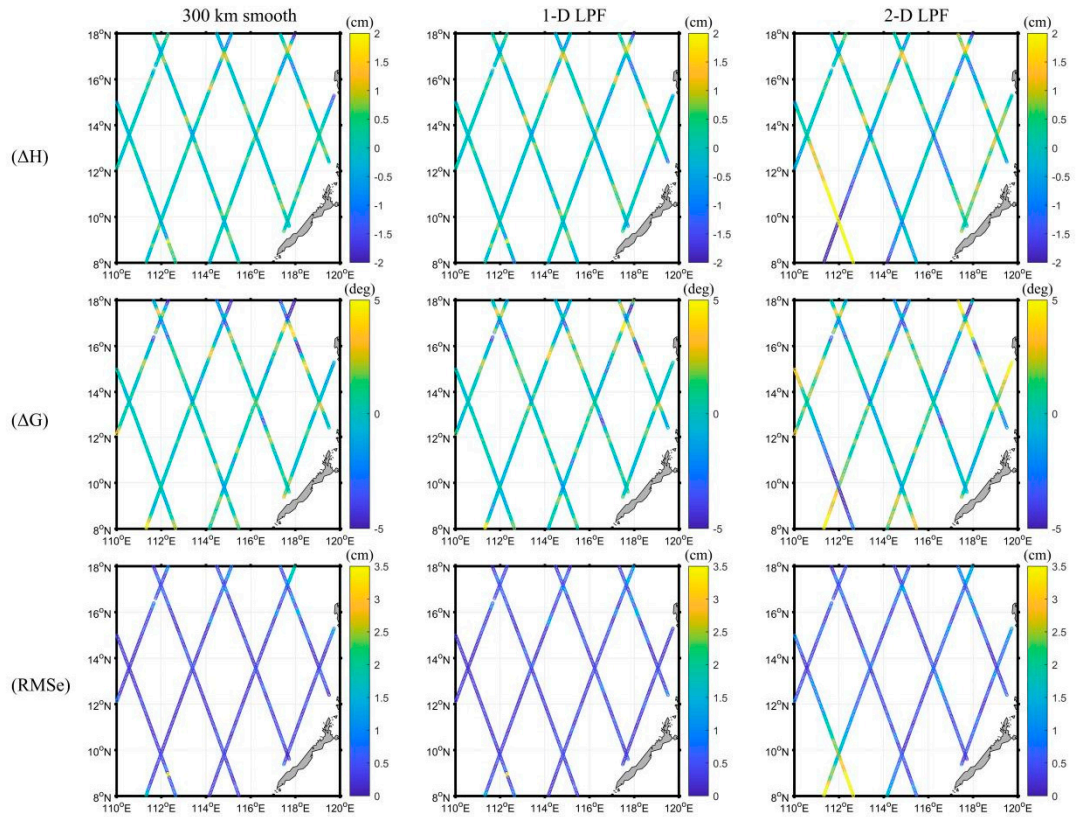**Figure S3**. Satellite altimeter amplitude data and phase lag data of M2 tidal constituent.

Figure S4. Amplitude changes (ΔH), phase lag changes (ΔG) and root mean square errors (RMSe) of the M2 internal tide acting on the sea surface extracted by 300 km smooth method (left part), 1-D LPF method (middle part) and 2-D LPF method (right part).
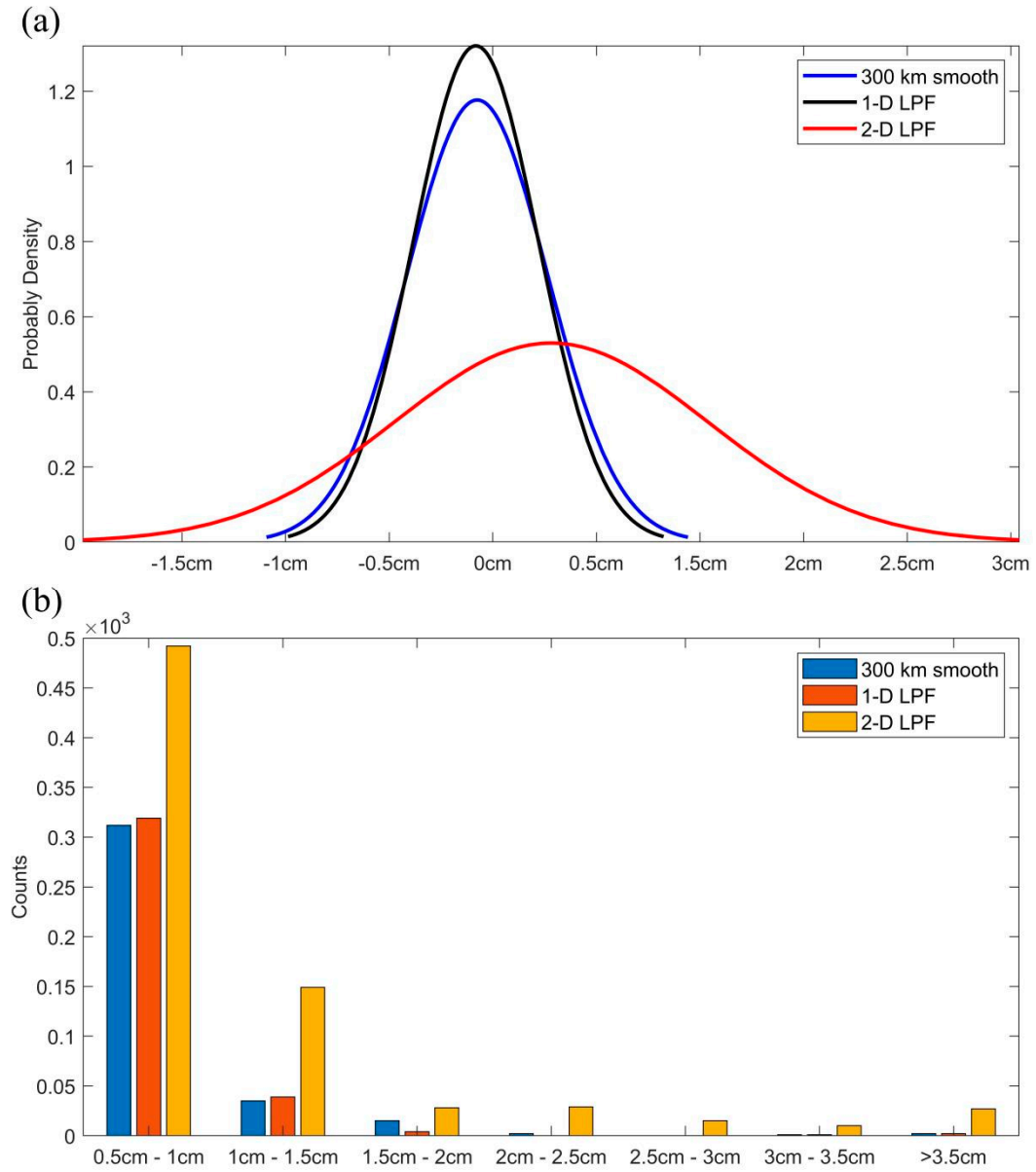
Figure S5. (a) The root mean square errors (RMSe) normal distribution plot of the 300 km smooth method, 1-D LPF method and 2-D LPF method. (b) Comparison of the count of the root mean square errors (RMSe) for the 300 km smooth method, 1-D LPF method and 2-D LPF method at different ranges.
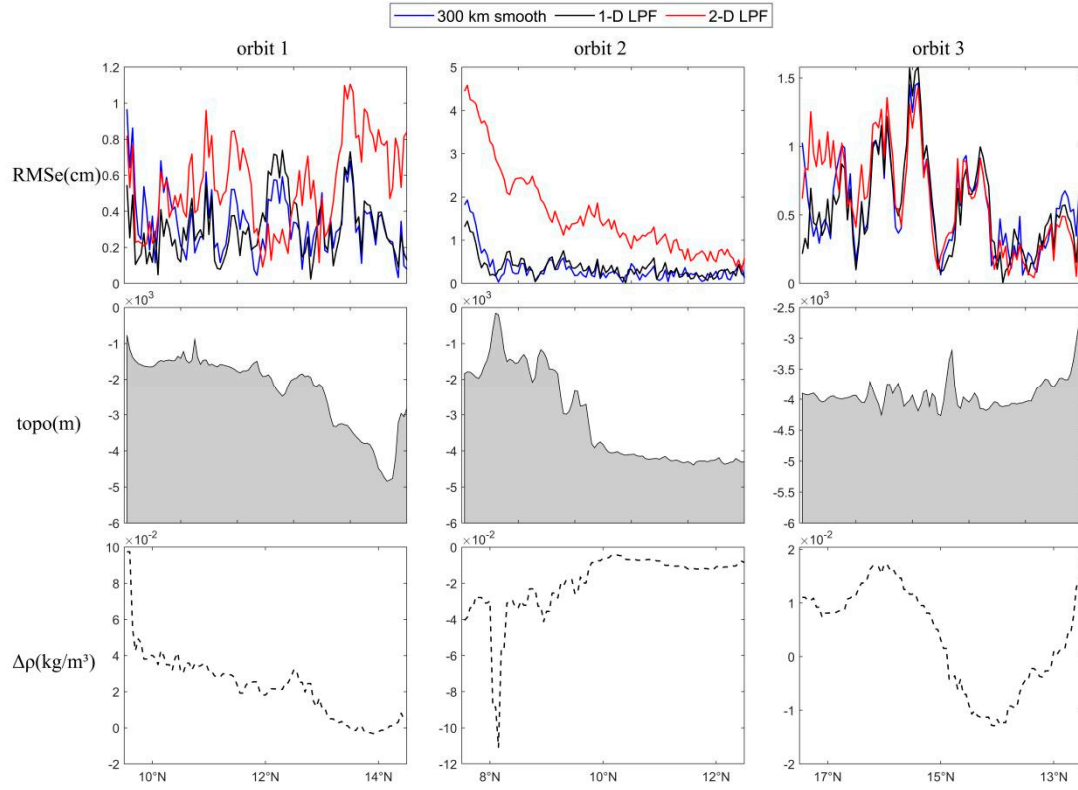
Figure S6. The RMSe, topography, and density perturbations obtained by 300 km smooth method, 1-D LPF method and 2-D LPF method for three orbits.

Table S1. The correlation coefficients between the RMSe derived from 300 km smooth method, 1-D LPF method, 2-D LPF method, and the topography and density perturbations.

r – topo	orbit 1	orbit 2	orbit 3
300 km smooth	0.045	0.291	-0.196
1-D LPF	-0.155	0.300	-0.184
2-D LPF	-0.369	0.421	-0.178
r – Δρ	orbit 1	orbit 2	orbit 3
300 km smooth	0.017	0.085	0.096
1-D LPF	-0.119	0.176	0.095
2-D LPF	-0.508	-0.213	0.214